Photovoltaic Devices with Methanofullerenes as Electron Acceptors

Junxin Li,† Na Sun, Zhi-Xin Guo,* Congju Li, Yongfang Li, Liming Dai, and Daoben Zhu

Institute of Chemistry, Chinese Academy of Sciences, Beijing 100080, China

Denkui Sun and Yong Cao

Institute of Polymer Opto-Electronic Materials and Devices, South China University of Technology, Guangzhou 510640, China

Louzhen Fan

Department of Chemistry, Beijing Normal University, Beijing 100875, China

Received: April 24, 2002; In Final Form: August 29, 2002

In this paper, the electrochemical and photophysical properties of two well-solubilized monofunctionalized methanofullerene derivatives (TDC_{60} and TC_{60}) were investigated by cyclic voltammetry, UV−visible absorption, and fluorescence spectroscopic methods. These two methanofullerenes show almost the same electron acceptor properties. The MEH-PPV/methanofullerene blends were made, and it was found that the photoluminescence of MEH-PPV could be quenched more efficiently by TDC_{60}. The two methanofullerenes were used to fabricate organic photovoltaic devices by taking MEH-PPV as the electron donor. Although the photovoltaic properties of the MEH-PPV/methanofullerene devices are better than those of the pristine MEH-PPV, the MEH-PPV/TDC_{60} device system shows even better performances. Considering the similarities of the structures as well as the electron acceptor abilities, the better performance of the MEH-PPV/TDC_{60} photovoltaic device should be due to the better compatibility of TDC_{60} with MEH-PPV, which was confirmed by AFM investigation.

1. Introduction

Photoinduced electron transfer between semiconducting conjugated polymers and fullerenes has recently attracted considerable scientific and technological attention. "Bulk heterojunction" polymer photovoltaic devices have been constructed by taking composite films of semiconducting polymer as electron donors and fullerene derivatives as electron acceptors.[1−8] The primary step in these polymer photovoltaic devices is an ultrafast photoinduced electron-transfer reaction at the donor−acceptor interface, which results in a metastable charge-separated state. The quantum efficiency of this step is assumed to be close to unity.[9,10] However, the overall conversion efficiency of these devices is limited by the carrier collection efficiency, which is greatly influenced by morphology,[1,2,4,11,12] e.g., phase separation, within the active film. Recently, more effort have been expended to improve the morphology of the active layer by design and synthesis of new conjugated polymers as well as polymer−fullerene dyads. For example, Zerza and Martín et al.[13] fabricated an organic photovoltaic device using a new cyano-substituted naphthalene−vinylene type conjugated polymer as the electron donor and the fullerene derivative 1-(3-(methoxycarbonyl)propyl)-1-phenyl-(6,6)-C_{61} (PCBM) as the electron acceptor. Nierengarten et al.[11] synthesized a series of fullerene−oligophenylenevinylene hybrids, and their systematic studies including electrochemical and photophysical properties as well as photovoltaic device performance reveal that the efficiency of the devices is limited by the fact that photoinduced electron transfer from the phenylenevinylene moiety to the C_{60} sphere must compete with an efficient energy transfer. Sariciftci and Janssen et al.[10] reported the photophysical properties and photovoltaic device performance of another series of oligo(*p*-phenylenevinylene) fullerene dyads.

SCHEME 1

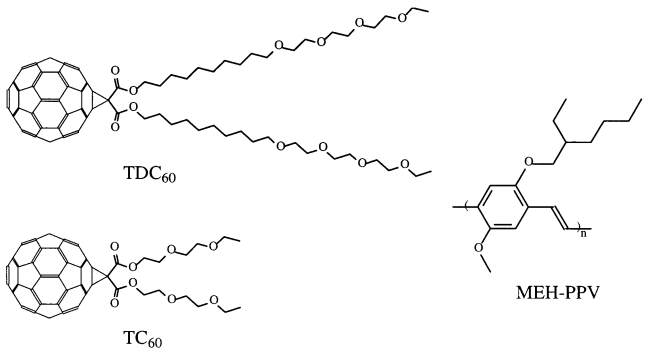

In this work we present a systematic investigation of the electrochemical and spectroscopic properties of two new monofunctionalized methanofullerene derivatives and the composites composed of methanofullerenes and the conjugated polymer poly((2-methoxy-5-((2-ethylhexyl)oxy)-1,4-phenylene)vinylene) (MEH-PPV). These two methanofullerenes have different chain structures (Scheme 1). TDC_{60} contains an inner hydrophobic part (decyl chain) and an outer hydrophilic part (triethylene glycols). TC_{60} is composed of only a hydrophilic part (triethylene glycol chain). Because of the long chain moieties, the two methanofullerenes show excellent solubility in a wide range of organic solvents including hexane, toluene, chloroform,

* Corresponding author. E-mail: gzhixin@infoc3.icas.ac.cn.
† Graduate School of the Chinese Academy of Sciences.

10.1021/jp025973v CCC: $22.00
Published on Web 10/10/2002

and methanol. Therefore, they are potential electronic acceptors and can be easily used to make organic photovoltaic devices. Photoinduced charge transfer was observed in the presence of these two methanofullerenes and MEH-PPV, respectively. It is further demonstrated that the TDC_{60}/MEH-PPV diodes show better photovoltaic performance because of the better morphology of the blend observed by atomic force microscopy.

2. Experiment

2.1. Materials. Methanofullerene derivatives were synthesized using Bingle's reaction.[14,15] MEH-PPV was synthesized according to the literature.[16] Tetrabutylammonium hexafluorophosphate ($TBAPF_6$) was purchased from Alfa Aecer and dried in a vacuum for about 6 h before use. Analytical grade dichloroform was dried over CaH_2 and distilled before use. Spectrophotometry grade organic solvents were used as received with criteria of no solvent interference on absorption and emission spectra in the wavelength region of interest.

2.2. Measurements. The electrochemical properties of fullerene derivatives were studied using cyclic voltammetry (CV), which was performed by a CHI-705 Chemical Analysis System in CH_2Cl_2 containing 0.1 M $TBAPF_6$ as the supporting electrolyte, with a polished Pt disk of 3 mm diameter as the working electrode, a Pt plate as the counter electrode, and a saturated calomel electrode (SCE) as the reference electrode. The concentration of samples was about 1×10^{-4} M. The experiments were performed at room temperature with a scan rate of 100 mV/s. Argon was purged through the working solution for 3 min for deaeration prior to experiments, and the argon gas was kept above the solution during the measurements.

Absorption spectra were obtained using a computer-controlled Shimadzu UV-2501PC UV−visible spectrophotometer. Emission spectra were recorded on a Spex Fluorolog-3 photon-counting emission spectrometer equipped with a 450 W xenon lamp, a Spex 600 grooves/mm dual-grating (blazed at 1000 nm) as the emission monochromator, and a 1200 grooves/mm grating (blazed at 600 nm) as the excitation monochromator. The detector is a thermoelectronically cooled detector that consists of a near-infrared-sensitive Hamamatsu R2658P photomutiplier tube operated at −1500 V. In fluorescence measurements a Schott 500 nm (KV 500) color glass sharp-cut filter was placed before the emission monochromator to eliminate the excitation scattering. Fluorescence spectra were corrected for nonlinear response by using a predetermined correction factor provided by the company. All of the experiments were done at room temperature.

A multimode Nanoscope III AFM controller (Digital Instrument, Santa Barbra, CA) and an ambient contact mode cantilever holder were used to measure the AFM images. The spring constant was 0.12 N/m. The scan rate was set to 2.5 Hz. Composite films of MEH-PPV/C_{60} derivatives from chloroform solution were spin cast on cleaved mica for the AFM studies.

Photovoltaic cells were fabricated in the anode/C_{60}-doped polymer/cathode single-layer structure. Blends of MEH-PPV with the two methanofullerenes were used as the active layer, respectively. The transparent anode is composed of an indium/tin oxide (ITO) layer coated with a 100 nm thick poly(ethylene dioxythiophene)/poly(tyrenesulfonic acid) (PEDOT/PSS) (Bayer, Batron-P 4083) layer. Incorporating a PEDOT/PSS layer between ITO and the active layer can reduce device leakage. The PEDOT/PSS layer was dried in a vacuum oven at 80 °C for 1 h. Organic photovoltaic devices were the photoactive polymer mixture (pristine MEH-PPV or MEH-PPV/methanofullerene (2:1, w/w)), which was cast by spin casting from a chloroform solution. The thickness of the MEH-PPV layer was 100 nm, as determined by the surface profiler (Tencor, Alfa-Step 500). The 150−250 nm thick aluminum was used as a cathode in this study. They were deposited by thermal deposition. The deposition rates and the thickness of the evaporation layers were monitored by a thickness/rate meter (Sycon, STM100). The deposition rates of Al were usually 0.5−1 nm/s. The cathode area defined the size of the active area as 0.15 cm^2. Except for spin-casting PEDOT/PSS layer, all the fabrication steps were carried out in a nitrogen glovebox. $I-V$ characteristics in the dark and under illumination were carried out with a computer-controlled Keithley Model 236 Source-Measure Unit. Illumination for the photovoltaic devices was provided by white light from the tungsten lamp with 100 mW/cm^2. The photocurrent of the photovoltaic devices was measured with a Merlin Digital Lock-in Radiometric System (Oriel Instruments with a Cornerstone 1301/8 M motorized monochromator and 100 W xenon lamp).

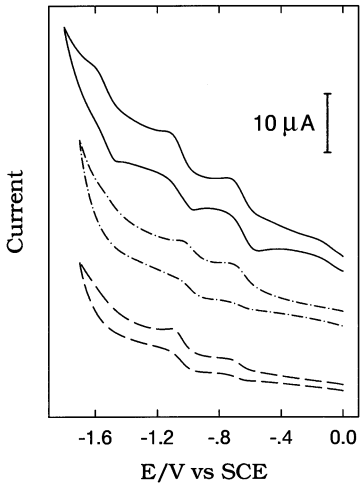

Figure 1. Cyclic voltammograms of C_{60} (—), TDC_{60} (− − −), and TC_{60} (−•−) on Pt in CH_2Cl_2 solution (using 0.1 M $TBAPF_6$ as supporting electrolyte) at room temperature.

3. Results

3.1. CV of TDC_{60} and TC_{60}. The electrochemical properties of the two methanofullerenes were studied by cyclic voltammetry at room temperature in dichloromethane solution using $TBAPF_6$ as the supporting electrolyte. The cyclic voltammograms of the methanofullerene derivatives show two similar quasi-reversible reduction waves in the potential range from 0.0 to −1.8 V, as shown in Figure 1. Their redox properties are similar to that of the parent C_{60} with a slightly negative shift of the half-wave potential of the first reduction process.

3.2. Photophysical Properties of TDC_{60} and TC_{60}. UV−visible absorption of the two methanofullerene derivatives was measured in room-temperature chloroform solution (Figure 2A). The spectral parameters are summarized in Table 1. The absorption spectra of the two derivatives are similar. Both of the methanofullerenes show the red onset absorption at ∼1.8 eV and also the maximum absorption peak at ∼2.6 eV. The fluorescence spectra were measured in room-temperature toluene solution. The emissions have a maximum at ∼1.76 eV with a shoulder peak at ∼1.6 eV (Figure 2B). The fluorescence quantum yields of TDC_{60} and TC_{60} in room-temperature solution ($\sim 4 \times 10^{-5}$ M) were determined quantitatively in reference to the yield of C_{70} ($\sim 4 \times 10^{-6}$ M).[17] Both TDC_{60} and TC_{60} have similar fluorescence yields higher than that of C_{60} (Table 1).

TABLE 1: Basic Redox and Photophysical Properties of TDC_{60} and TC_{60} Compared with C_{60}[a]

	E_1 (V)	E_2 (V)	Abs_{0-0} (nm)	ϵ_{0-0} ($M^{-1}\cdot cm^{-1}$)	Abs_{max} (nm)	ϵ_{max} ($M^{-1}\cdot cm^{-1}$)	$FLSC_{0-0}$ (eV)	$10^{-4}\phi_F$
C_{60}[b]	−0.65	−1.05					1.70	3.2
TDC_{60}	−0.67	−1.02	689	213	470	2530	1.76	5.1
TC_{60}	−0.67	−0.97	688	207	477	2160	1.76	5.7

[a] Half-wave potentials were measured in CH_2Cl_2; absorption properties were measured in $CHCl_3$, and fluorescence properties were measured in toluene. [b] Absorption measured in toluene.

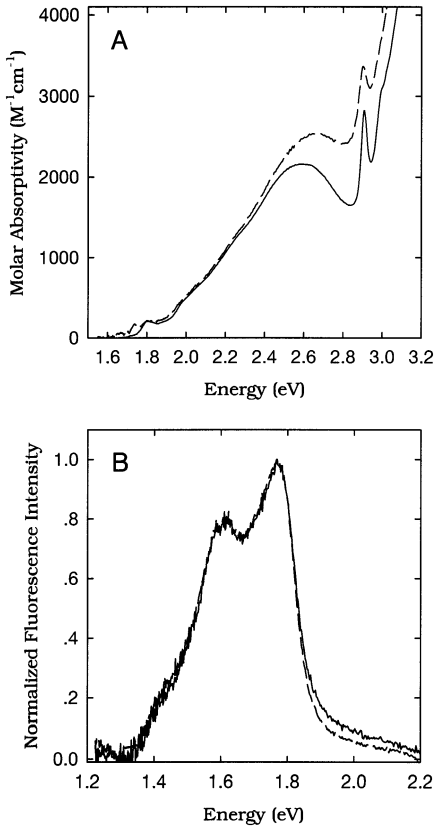

Figure 2. Absorption (A) (in chloroform) and fluorescence spectra (B) (in toluene) of TDC_{60} (− − −) and TC_{60} (—). Fluorescence spectra were recorded at room temperature by excitation at 2.6 eV (470 nm).

3.3. Photoluminescence Quenching. To study the photoluminescence quenching of the MEH-PPV/methanofullerene composite films, the pristine MEH-PPV or MEH-PPV/methanofullerene (2:1, w/w) in chloroform solution was spin cast on glass with an average thickness of ∼100 nm. The room-temperature fluorescence spectrum of a pristine film of MEH-PPV is shown in Figure 3, together with the photoluminescence of the MEH-PPV/methanofullerene composite films measured at the same conditions. The luminescence of MEH-PPV shows a rather broad peak centered at ∼2.1 eV. This is in agreement with the literature reported before.[18] The intense photoluminescence of the MEH-PPV is quenched significantly by doping of TDC_{60} or TC_{60}. TDC_{60} is obviously a better quencher than TC_{60}.

3.4. AFM. The AFM images obtained for the composite films of MEH-PPV/methanofullerene are shown in Figure 4. It is clear that the AFM image of MEH-PPV/TDC_{60} reveals a continuous film with slight roughness and some small islands with a height of less than 2 nm. However, the AFM image of the MEH-PPV/TC_{60} film shows an obviously large roughness and some large islands with a height of around 9 nm. These results imply that TDC_{60} is more compatible with MEH-PPV than TC_{60}.

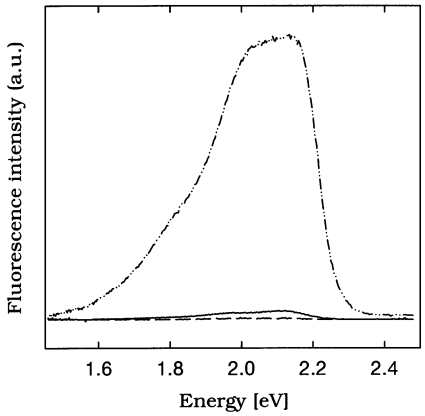

Figure 3. Fluorescence spectra of MEH-PPV (−••−), MEH-PPV/TDC_{60} (− − −), and MEH-PPV/TC_{60} (—) (2/1, w/w) spin cast films. Data were recorded at room temperature by excitation at 3.1 eV (400 nm).

TABLE 2: Photovoltaic Characteristics of MEH-PPV Based Photovoltaic Devices

active layer	V_{oc} (V)	I_{sc} ($mA\cdot cm^{-2}$)	IPCE (%)	η_e (%)	FF
MEH−PPV/TDC_{60}	0.70	0.053	5.91 (525 nm)	0.49	0.26
MEH−PPV/TC_{60}	0.70	0.065	1.89 (515 nm)	0.22	0.39
MEH−PPV	1.05	0.00059	0.081(530 nm)	0.071	0.19

3.5. Photovoltaic Devices. Organic photovoltaic devices were fabricated from MEH-PPV/methanofullerene (2/1, w/w) solutions as described in the experimental section. Figure 5 shows the $I-V$ curves of the photovoltaic devices fabricated from pristine MEH-PPV and MEH-PPV sensitized with TDC_{60} and TC_{60}. The solar cell parameters such as open circuit voltage V_{oc}, short circuit current I_{sc}, fill factor FF, and energy conversion efficiency η_e are given in Table 2.

Whereas the pristine MEH-PPV photovoltaic device shows a high open circuit voltage (1.05 V), low short circuit current (0.59 $\mu A\cdot cm^{-2}$), low fill factor (0.19), low energy conversion efficiency (0.071%), and rectification of 13 at ±2 V and 118 at ±3 V, the TDC_{60} and TC_{60} sensitized photovoltaic devices show better photovoltaic performance, respectively. The characteristic data of the TC_{60} sensitized MEH-PPV photovoltaic device are an open circuit voltage of 0.70 V, a short circuit current of 65 $\mu A\cdot cm^{-2}$, a fill factor of 0.39, and a power conversion efficiency of 0.22%. The rectification of this device is ∼1320 at ±2 V and ∼480 at ±3 V in the dark. The dark $I-V$ curve shows a small change in the curvature at 0.5 V. Between −0.5 and +0.5 V the logarithmically plotted dark current is rather symmetric to the 0 V center for positive and negative applied voltages. The TDC_{60} sensitized photovoltaic device shows an open circuit voltage of 0.70 V, a short circuit current of 53 $\mu A\cdot cm^{-2}$, an energy fill factor of 0.39, and a power conversion efficiency of 0.49%. The rectification of this device is ∼50 at ±2 V and ∼160 at ±3 V in the dark. The dark $I-V$ curve shows a small change in the curvature at 0.8 V. Just like the TC_{60} sensitized solar cell, between −0.8 and +0.8 V the logarithmically plotted

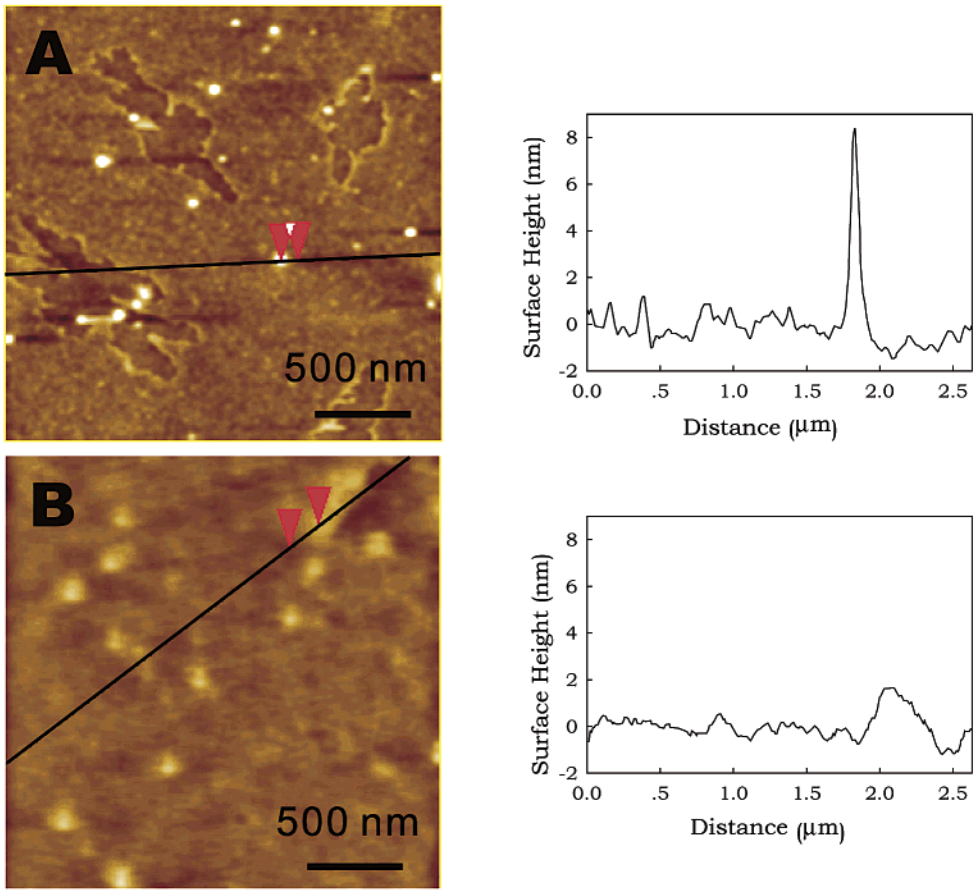

Figure 4. AFM images showing the surface morphology of (A) MEH-PPV/TC_{60} (2/1, w/w) and (B) MEH-PPV/TDC_{60} (2/1, w/w) composite films spin cast from chloroform solution on mica.

dark current is rather symmetric to the 0 V center for positive and negative applied voltages.

Figure 6 compares the spectrally resolved photocurrent of the pristine MEH-PPV (A), MEH-PPV/TC_{60} (B), and MEH-PPV/TDC_{60} (C) photovoltaic devices together with the absorption spectra of thin films spin-cast on glass with comparable thickness. The incident photon to converted electron efficiency (IPCE) was calculated from the spectrally resolved short-circuit current by the following formula

$$\text{IPCE (\%)} = \frac{1240}{\lambda\ (\text{nm})} \cdot \frac{I_{sc}\ (\mu A/\text{cm}^2)}{I_{inc}\ (\text{W/m}^2)}$$

where I_{inc} is the intensity of the incident light. The peak values are listed in Table 2.

All three IPCE curves have the same onset (~2.1 eV) as well as the same spectrally resolved maximum, which is typical for low optical density cells. Whereas the pristine MEH-PPV shows a maximum IPCE of 0.08% at 2.34 eV, the MEH-PPV/TC_{60} shows the corresponding IPCE value of 1.89% at 2.41 eV, and the IPCE value of MEH-PPV/TDC_{60} is 5.91% at 2.36 eV, 70 times higher than that of the pristine MEH-PPV. The peak energy conversion efficiencies of the device are 0.07% for the pristine MEH-PPV diodes (2.34 eV), 0.22% for the TC_{60}/MEH-PPV diodes (2.41 eV), and 0.49% for the TDC_{60}/MEH-PPV diodes (2.36 eV), respectively.

4. Discussion

TDC_{60} and TC_{60} essentially retain the cathodic electrochemical pattern of the parent fullerene. The reduction potentials of all these species shift to more negative values when compared with those of pure C_{60}. This is the classical behavior observed for all methanofullerene derivatives,[19] whose cyclic voltammetry is typically characterized by small shifts to more negative potentials as the electron affinities of the fullerene derivatives decrease with decreasing electron negativities of the attached atoms and the saturation of a double bond on the C_{60} surfaces, which raises the LUMO energy.[11,19]

TDC_{60} and TC_{60} exhibit similar absorption and fluorescence properties, which are also similar to those of other methanofullerenes reported before.[20−22] As the alkyl or alkoxy functional groups attached to the fullerene cage have little effect on the electronic structure of the fullerene moiety, the photophysical properties of these C_{60} derivatives should be dictated by the fullerene cage that is monosubstituted through a [6,6] closed methano addition pattern. Thus these two methanofullerenes investigated should show similar photophysical properties. The similarity of the photophysical properties together with the similarity of the redox properties of the TDC_{60} and TC_{60} implies that these two compounds should have very similar acceptor properties.

The two methanofullerenes can quench the luminescence of MEH-PPV sufficiently, indicating a rapid photoinduced charge transfer in the bulk of MEH-PPV/methanofullerene composites, as observed for other PPV/fullerene blends.[10−13, 23] Although TDC_{60} and TC_{60} have very similar acceptor properties, which have been verified by electrochemical studies, the quenching ability of the two methanofullerenes to the photoluminescence of MEH-PPV is different. The TDC_{60} is a better quencher than TC_{60}. In solid films, the photoluminescence quenching not only depends on the acceptor ability of the quencher but also is highly

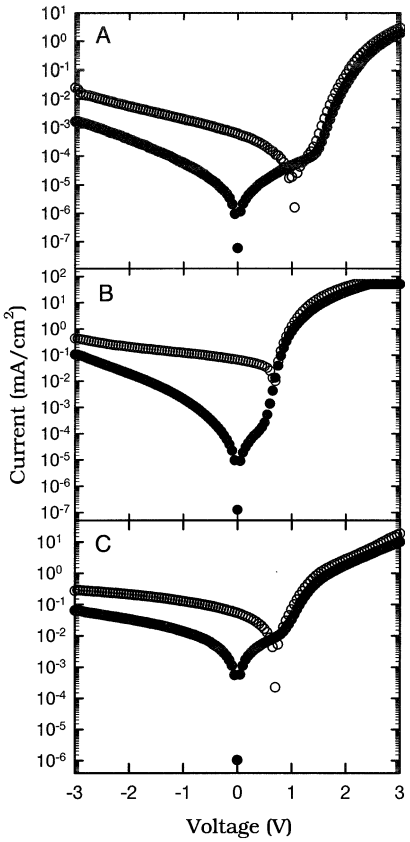

Figure 5. Semilogarithmic plot of the $I-V$ characteristics of three photovoltaic devices with a spin cast film of MEH-PPV (A), MEH-PPV/TC_{60} (B), and MEH-PPV/TDC_{60} (C) as an active layer between an ITO front electrode and an Al back electrode under illumination (○) and in the dark (●).

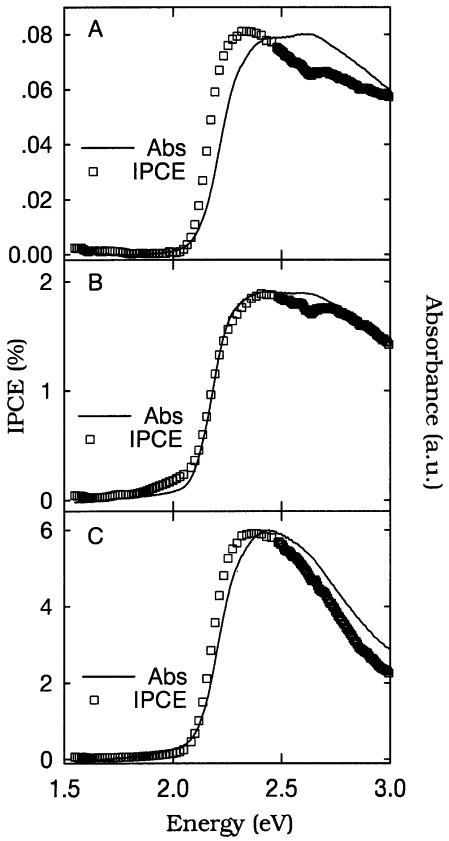

Figure 6. Incident photon to converted electron efficiency (□) plot of three photovoltaic devices with spin cast film of MEH-PPV (A), MEH-PPV/TC_{60} (B), and MEH-PPV/TDC_{60} (C) as an active layer between an ITO front electrode and an Al back electrode and absorption (—) plot of these spin cast films on glass.

related to the morphology (e.g., compatibility of the two species) of the composites. In our system investigated, the donor is the same (MEH-PPV), and the electron acceptors' ability is also the same. The present quenching results imply a logical conclusion that TDC_{60} is more compatible with MEH-PPV. This is in agreement with the AFM results.

In the $I-V$ curves of pristine MEH-PPV, MEH-PPV/TDC_{60}, and MEH-PPV/TC_{60} photovoltaic devices, the logarithmically plotted photocurrent is rather symmetric to the 0 V center between a certain range of positive and negative applied voltages, respectively. Such symmetry can be explained by the contribution of a small shunt resistivity to the photocurrent, which manifests as "ohmic" behavior in the low current regime of a diode. For all of the photovoltaic devices, the dark current and the photocurrent are comparable to each other at higher forward bias, indicating that photoconductivity does not play an important role for these devices. Upon addition of methanofullerenes, about a 100-fold increase in the short circuit current is observed. This is in agreement with data for the fullerene/PPV diodes reported before.[24] It was reported by Brabec et al.[25] recently that the open circuit voltage of conjugated polymer/fullerene bulk-heterojunction solar cells is directly related to the acceptor strength of the fullerenes. In this work, the two fullerene derivatives are methanofullerenes that have the same electrochemical active moiety (C_{60} moiety) as PCBM, and their open circuit voltages are also similar.

From Figure 5 it can be seen clearly that there is perfect symmetrical behavior for both the TC_{60} and TDC_{60} doped MEH-PPV diodes. This is a strong indication for direct charge generation within the whole absorptive region as well as for rather balanced hole and electron mobilities. The IPCE value can be greatly increased upon addition of methanofullerenes. The IPCE value of the TDC_{60}/MEH-PPV diode is 3 times as large as that of the TC_{60}/MEH-PPV diode.

The $I-V$ and IPCE studies for MEH-PPV photovoltaic devices with different acceptors discussed above already give indications that the photovoltaic conversion efficiency is strongly related to the interpenetrating network morphology for bipolar devices. Although the electrochemical and photophysical properties of TDC_{60} and TC_{60} have little difference, the photovoltaic devices doped with these two methanofullerenes are different in energy conversion efficiency and IPCE value. This implies that the TDC_{60} has better compatibility with MEH-PPV, which was strongly supported by the morphology studies of the composite films from AFM. Comparing the structures of the two fullerene derivatives, TDC_{60} has a decyl chain, which connects the hydrophilic triethylene glycol moiety to fullerene. This makes TDC_{60} more flexible and more hydrophobic than TC_{60} and results in photovoltaic performances better than those of TC_{60}.

5. Conclusion

Two new monofunctionalized methanofullerene derivatives were used to fabricate organic photovoltaic devices with MEH-PPV. The electrochemical and photophysical properties of these methanofullerene derivatives were well-characterized using CV, UV−visible, and fluorescence spectroscopic methods. The CVs of both TDC_{60} and TC_{60} show almost the same quasi-reversible reduction waves in the measured potential range. The two methanofullerenes also exhibit similar absorption and fluores-

cence properties. These results suggest that the different chains covalently attached to the C_{60} sphere do not influence their electronic properties and the two compounds investigated have very similar electron acceptor properties. However, the photoluminescence of MEH-PPV could be quenched more efficiently by TDC_{60} compared with that of TC_{60}. The photovoltaic devices were fabricated by the combination of MEH-PPV with methanofullerenes and compared with the pristine MEH-PPV device. Both of the methanofullerene doped photovoltaic devices show better photovoltaic performance, with the MEH-PPV/TDC_{60} system showing even better results than MEH-PPV/TC_{60}. The photoluminescence quenching results together with the photovoltaic device studies imply that TDC_{60} is more compatible with MEH-PPV than TC_{60}. This deduction is confirmed by the AFM studies, which indicate that the morphology of MEH-PPV/TDC_{60} is much better than that of MEH-PPV/TC_{60}. Further work will be focused on the increasing energy conversion efficiency through the understanding of the morphology of fullerene derivatives with conjugated polymers.

Acknowledgment. We thank the Chinese Academy of Sciences and the Major State Basic Research Development Program (Grand No. G2000077500) for financial support.

References and Notes

(1) Brabec, C. J.; Sariciftci, N. S.; Hummelen, J. C. *Adv. Funct. Mater.* **2001**, *11*, 15.
(2) Brabec, C. J.; Sariciftci, N. S. *Monatsh. Chem.* **2001**, *132*, 421.
(3) Halls, J. J. M.; Walsh, C. A.; Greenham, N. C.; Marseglia, E. A.; Friend, R. H.; Moratti, S. C.; Holmes, A. B. *Nature* **1995**, *376*, 498.
(4) Yu, G.; Gao, J.; Hummelen, J. C.; Wudl, F.; Heeger, A. J. *Science* **1995**, *270*, 1789.
(5) Yu, G.; Heeger, A. J. *J. Appl. Phys.* **1995**, *78*, 4510.
(6) Granström, M.; Petrisch, K.; Arias, A. C.; Lux, A.; Lux, M.; Andersson, M. R.; Friend, R. H. *Nature* **1998**, *395*, 257.
(7) Brabec, C. J.; Cravino, A.; Zerza, G.; Sariciftci, N. S.; Kiebooms, R.; Vanderzande, D.; Hummelen, J. C. *J. Phys. Chem. B* **2001**, *105*, 1528.
(8) Zhang, F.; Svensson, M.; Andersson, M. R.; Maggini, M.; Bucella, S.; Menna, E.; Inganäs, O. *Adv. Mater.* **2001**, *13*, 1871.
(9) Ouali, L.; Krasnikov, V. V.; Stalmach, U.; Hadziioannou, G. *Adv. Mater.* **1999**, *11*, 1515.
(10) Peeters, E.; van Hal, P. A.; Knol J.; Brabec, C. J.; Sariciftci, N. S.; Hummelen, J. C.; Janssen, R. A. J. *J. Phys. Chem. B* **2000**, *104*, 10174.
(11) Eckert, J.-F.; Nicoud, J.-F.; Nierengarten, J.-F.; Liu, S.-G.; Echegoyen, L.; Barigelletti, F.; Armaroli, N.; Ouali, L.; Krasnikov, V.; Hadziioannou, G. *J. Am. Chem. Soc.* **2000**, *122*, 7467.
(12) Gu, T.; Nierengarten, J.-F. *Tetrahedron Lett.* **2001**, *42*, 3175.
(13) Zerza, G.; Röthler, B.; Sariciftci, N. S.; Gómez, R.; Segura, J. L.; Martín, N. *J. Phys. Chem. B* **2001**, *105*, 4099.
(14) Sun, N.; Wang, Y.; Song, Y.; Guo, Z.; Dai, L.; Zhu, D. *Chem. Phys. Lett.* **2001**, *344*, 277.
(15) Sun, N.; Guo, Z.; Li, J.; Dai, L.; Zhu, D. Unpublished results.
(16) Hsieh, B. R.; Yu, Y.; Vanlaeken, A. C.; Lee, H. *Macromolecules* **1997**, *30*, 8097.
(17) Ma, B.; Sun, Y.-P. *J. Chem. Soc., Perkin. Trans. 2*, **1996**, 2157.
(18) Jakubiak, R.; Rothberg, L. J.; Wan, W.; Hsieh, B. R. *Synth. Met.* **1999**, *101*, 230.
(19) Suzuki, T.; Maruyama, Y.; Akasaka, T.; Ando, W.; Kobayashi, K.; Nagase, S. *J. Am. Chem. Soc.* **1994**, *116*, 1359.
(20) Sun, Y.-P.; Gurudu, R.; Lawson, G. E.; Mullins, J. E.; Guo, Z.; Quinlan, J.; Bunker, C. E.; Gord, J. R. *J. Phys. Chem. B* **2000**, *104*, 4625.
(21) Ma, B.; Bunker, C. E.; Guduru, R.; Zhang, X.-F.; Sun, Y.-P. *J. Phys. Chem. A* **1997**, *101*, 5626.
(22) Guldi, D. M.; Hungerbúhler, H.; Carmichael, I.; Asmus, K.-D.; Maggini, M. *J. Phys. Chem. A* **2000**, *104*, 8601.
(23) van Duren, J. K. J.; Dhanabalan, A.; van Hal, P. A.; Janssen, R. A. J. *Synth. Met.* **2001**, *121*, 1587.
(24) Gao, J.; Hide, F.; Wang, H. L. *Synth. Met.* **1997**, *84*, 979.
(25) Brabec, C. J.; Cravino, A.; Meissner, D.; Sariciftci, N. S.; Fromherz, T.; Rispens, M. T.; Sanchez, L.; Hummelen, J. C. *Adv. Funct. Mater.* **2001**, *11*, 374.